

The dependence of maximum starspot amplitude and the amplitude distribution on stellar properties

Steven H. Saar¹, Michelle Dyke^{1,2}, Søren Meibom¹ and Sydney A. Barnes³

¹Smithsonian Astrophysical Obs.,
60 Garden Street, Cambridge, MA 02138, USA
email: saar@cfa.harvard.edu, smeibom@cfa.harvard.edu

²Yale Univ. New Haven, CT USA

³Lowell Obs., 1400 W. Mars Hill Road, Flagstaff, AZ 86011
email: barnes@lowell.edu

Abstract. We combine photometric data from field stars, plus over a dozen open clusters and associations, to explore how the maximum photometric amplitude (A_{\max}) and the distribution of amplitudes varies with stellar properties. We find a complex variation of A_{\max} with inverse Rossby number Ro^{-1} , which nevertheless can be modeled well with a simple model including an increase in A_{\max} with rotation for low Ro^{-1} , and a maximum level. A_{\max} may then be further affected by differential rotation and a decline at the highest Ro^{-1} . The distribution of A_{spot} below A_{\max} varies with Ro^{-1} : it peaks at low A_{spot} with a long tail towards A_{\max} for low Ro^{-1} , but is more uniformly distributed at higher Ro^{-1} . We investigate further dependences of the A_{spot} distributions on stellar properties, and speculate on the source of these variations.

Keywords. Stars: spots, stars: rotation, stars: magnetic fields, stars: late-type, stars: evolution

1. Introduction and observations

A number of extensive photometric studies of open clusters and associations have been completed recently. Since the major compilation and study of spot amplitudes A_{spot} was by Messina *et al.* (2001), it is timely to revisit the dependence of A_{spot} (indicative of starspots) on other stellar properties, informed by the new data and other recent results (e.g., on differential rotation). We have collected photometric V amplitude and rotation period P_{rot} data from a large number of sources (Table 1) and made new fits to the light curves for two clusters (M35, NGC 3532). The total data set includes over 1200 stars with ages ranging from 10 Myr to roughly solar. We include only single stars or well separated binaries to avoid complications due to tidal/magnetic interactions, and difficulties in assigning amplitudes to a particular component. We also restrict ourselves to V data, which are more numerous (sadly, eliminates some recent cluster surveys).

2. Analysis and models

Based on Messina *et al.* (2001) we expect A_{spot} to depend on both rotation and mass. A simple, physically motivated parameterization for this is the inverse Rossby number $Ro^{-1} = \tau_C \Omega$ (where τ_C is the convective turnover timescale); the mean-field $\alpha\Omega$ dynamo

Table 1. Sources of A_{spot} data

Source	N_{star}	Age [Myr]	reference
β Pic assoc.	17	10	Messina <i>et al.</i> (2010b)
Tuc/Hor assoc.			
Col assoc.	52	30	Messina <i>et al.</i> (2010b)
Car assoc.			
NGC 2391	16	40	Patten & Simon(1996)
NGC 2602	29	40	Barnes <i>et al.</i> (1999)
IC 4665	8	40	Allain <i>et al.</i> (1996)
α Per	42	70	Messina <i>et al.</i> (2001) ¹
Pleiades	57	100	Messina <i>et al.</i> (2001) ¹
AB Dor group	32	100	Messina <i>et al.</i> (2010b)
M35	218	150	Meibom <i>et al.</i> (2009)
M11	8	215	Messina <i>et al.</i> (2010a)
NGC 3532	73	300	Barnes(2003) ²
M37	504	550	Hartman <i>et al.</i> (2009)
Coma	39	600	Collier Cameron <i>et al.</i> (2009)
Hyades	21	600	Messina <i>et al.</i> (2001) ¹
field	99	300-4000	Messina <i>et al.</i> (2001) ¹

Notes: ¹Data compilation (see references for original source); ² P_{rot} source, we measure A_{spot} for the first time.

number is proportional to Ro^{-2} , and Ro^{-1} figures prominently in stellar activity and rotational evolution (e.g., Barnes & Kim 2010). We take τ_C from Gunn *et al.* (1998).

Since A_{spot} is a relative measure, yielding the peak *difference* in spot coverage over rotation, we expect that the maximum A_{spot} seen at a given Ro^{-1} , A_{max} , will be the most indicative diagnostic of the true strength of dynamo-driven spot generation at that rotation rate. We study A_{max} (Fig. 1), the binned $A_{\text{spot}}(\text{Ro}^{-1})$ distributions, and moments thereof (Fig. 2).

If A_{max} behaves like other magnetic activity diagnostics (e.g., X-ray emission), we expect to see an increase in A_{max} with rotation at lower Ro^{-1} , a possible maximal "saturated" spottedness level above some critical Ro^{-1} , and a possible decrease in A_{max}

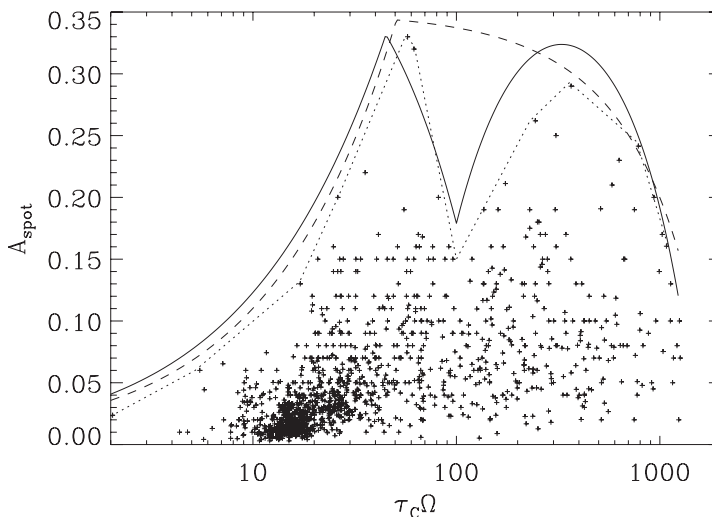


Figure 1. A_{spot} vs. Ro^{-1} for our sample (Table 1). The dashed line connects local A_{spot} maxima (A_{max}); the dashed and solid lines gives our approximate models (1 and 2, respectively) for A_{max} (see discussion).

again at very fast rotation rates (e.g., analogous to the “super-saturation” seen in coronae; e.g., Randich 1998). Causes for the latter phenomena are much debated, and part of the reason for such a study. Saturation may result from maximum surface coverage by fields/spots, Coriolis force-driven concentration of spots at poles, maximum dynamo output limited by back-reaction of magnetic fields on flows. A decline at the highest Ro^{-1} may be due to a continuation of the above, or simply due to lack of additional surface area to permit higher levels of inhomogeneity.

Connecting the highest observed $A_{max}(Ro^{-1})$ (Fig. 1, dotted line) does indeed show a general rise in A_{max} at lower Ro^{-1} , and a decrease at the highest Ro^{-1} . For intermediate values, however, the situation is less clear. One *could* more coarsely follow $A_{max}(Ro^{-1})$, and connect A_{max} high points at $Ro^{-1} \approx 60$ and 350, making a fairly smooth, though gently declining “saturated” A_{max} level. Alternatively, connecting A_{max} as indicated in Figure 1 shows a large “wedge” removed, with local minimum at $Ro^{-1} \approx 100$.

We have tried to construct simple models to match both of these scenarios. The first (“no-wedge”) $A_{max}(Ro^{-1})$ curve is well fit by:

$$A_{max} = \min\{a_1 Ro^{-b_1}; c_1(2 - e^{d_1/Ro})\} \tag{Model 1}$$

where $a_1, b_1, c_1,$ and d_1 are adjustable constants. This model contains both a power law increase in A_{max} , limited by a gradually decaying “saturation” level (the exponential term). The $A_{max}(Ro^{-1})$ curve with the “wedge” removed, can, surprisingly be fit by adding only one additional parameter:

$$A_{max} = \min\{a_2 Ro^{-b_2}; c_2(2 - e^{d_2/Ro})\} - f_2 \Delta\Omega \tag{Model 2}$$

where $a_2, b_2, c_2, d_2,$ and f_2 are adjustable constants, and $\Delta\Omega$ is the empirical relationship between surface differential rotation (DR) and Ro^{-1} for single dwarfs (Saar 2009; 2010, this volume). The latest fits for this yield $\Delta\Omega \propto Ro^{-1.00}$ for $Ro^{-1} < 100$ and $\Delta\Omega \propto Ro^{1.28}$ for $Ro^{-1} > 100$ (Saar 2010, this volume).

We also binned the A_{max} data into 12 bins of equal numbers in each (100 stars). We also studied the resulting distributions in each bin. Maxima and moments of these distributions are shown in Fig. 2.

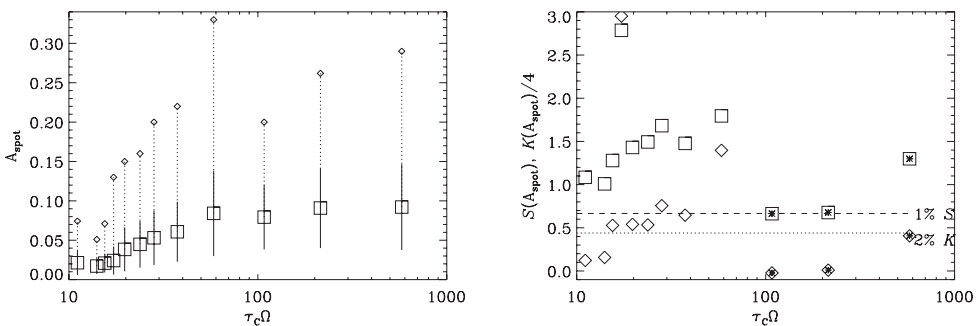


Figure 2. [Left]: The mean (boxes), $\pm\sigma$ width (solid), and maximum (diamonds) of the $A_{spot}(Ro^{-1})$ distribution in each of 12 bins with 100 stars in each. All three increase fairly steadily until the coronal saturation point ($Ro^{-1} \approx 100$). The mean A_{spot} also saturates here, while A_{max} and the distribution σ retreat, only to resume increasing towards higher Ro^{-1} . [Right]: Skewness S (boxes) and excess kurtosis $K/4$ (diamonds) of the $A_{spot}(Ro^{-1})$ distributions in 100 star bins. Similar to the distribution σ width (at left), S and K both increase with Ro^{-1} below saturation ($Ro^{-1} \approx 100$), whereafter they sharply decline (symbols marked with *). The 1% significance level for S (dashed) and 2% level for K (dotted) are also indicated.

3. Results and conclusions

We interpret the success of the added DR term as arising from the effect of strong shear on spot groups, smearing out the spot concentrations (and shredding the spots themselves), inevitably leading to more uniform spatial distributions and lower A_{\max} . The shearing effect of DR reaches a peak in a range of rapid rotators near the start of the “saturated activity” branch (where, e.g., L_X/L_{bol} reaches a constant maximum of $\approx 10^{-3}$). The sharp increase in A_{\max} for $\text{Ro}^{-1} > 100$ (Fig. 1) echoes the Messina *et al.* (2001) result, which we suggest is due to decreasing rotational shear in these stars, permitting larger spots, spot groups, and thence larger A_{\max} .

There are also a significant changes in A_{spot} distribution around $\text{Ro}^{-1} \sim 100$: it becomes narrower (Fig. 2, left), and markedly less skewed and more Gaussian (excess kurtosis $K \rightarrow 0$; Fig. 2, right) even while $\langle A_{\text{spot}} \rangle$ stays roughly constant (Fig. 2, left). These changes, occurring precisely at the local A_{\max} minimum, lends weight to the “wedged” interpretation of A_{\max} . Again, high shear should tend to smear out spot groups and structures, making distributions more homogeneous and reducing their moments.

Modeling and further observations are needed to help understand the physical processes underlying these results. Stronger Coriolis forces at high Ro^{-1} will drive increased flux emergence towards the poles (e.g., Schüssler & Solanki 1992), but spots are still observed to appear at all latitudes (e.g., Strassmeier 2009), suggesting a source of flux/spots nearer the surface. The implied increase in importance of a convection zone-based dynamo at higher Ro^{-1} (vs. a tachocline-driven one) is probably an important factor driving changing spot distributions, as are altered velocity fields (e.g., DR, meridional flows). Is there any significance to the sharp spike in S and K near $\text{Ro}^{-1} \approx 17$? Is there any relationship between coronal “super-saturation” and the drop in A_{\max} at high Ro^{-1} ? Do true spot areas continue increasing, even as $\langle A_{\text{spot}} \rangle$ saturates and A_{\max} declines? Indeed, *does* A_{\max} decline sharply? (The drop is not apparent in the binned data; Fig. 2, left.) More A_{spot} data at high Ro^{-1} , and measurements of absolute spot coverage using molecular bands (e.g., O’Neal *et al.* 1996; Saar *et al.* 2001) could be used to probe these issues. We are also beginning to explore some of these questions with simple models.

Acknowledgement

This work was supported by Chandra grants GO8-9025A and GO0-11041A.

References

- Allain, S., Bouvier, J., Prosser, C., Marschall, L. A., & Laaksonen, B. D. 1996, *A&A*, 305, 498
 Barnes, S. A. & Kim, Y.-C. 2010, *ApJ*, 721, 675
 Barnes, S. A. 2003, *ApJ*, 586, 464
 Barnes, S. A., Sofia, S., Prosser, C. F., & Stauffer, J. R. 1999, *ApJ*, 516, 263
 Collier Cameron, A., *et al.* 2009, *MNRAS*, 400, 451
 Gunn, A. G., Mitrou, C. K., & Doyle, J. G. 1998, *MNRAS*, 296, 150
 Hartman, J. D., *et al.* 2009, *ApJ*, 691, 342
 Meibom, S., Mathieu, R. D., & Stassun, K. G. 2009, *ApJ*, 695, 679
 Messina, S., Desidera, S., Turatto, M., Lanzafame, A. C., & Guinan, E. F. 2010, *arXiv:1004.1959*
 Messina, S., Parihar, P., Koo, J.-R., Kim, S.-L., Rey, S.-C., & Lee, C.-U. 2010, *A&A*, 513, A29
 Messina, S., Rodonò, M., & Guinan, E. F. 2001, *A&A*, 366, 215
 O’Neal, D., Saar, S. H., & Neff, J. E. 1996, *ApJ*, 463, 766
 Patten, B. M. & Simon, T. 1996, *ApJS*, 106, 489

- Randich, S. 1998, 10th Cool Stars, Stellar Systems, and the Sun, *ASP Conf. Ser.*, 154, 501
- Saar, S. H. 2009, Astronomical Society of the Pacific Conference Series, *ASP Conf. Ser.* 416, 375
- Saar, S. H., Peterchev, A., O'Neal, D., & Neff, J. E. 2001, 11th Cambridge Workshop on Cool Stars, Stellar Systems and the Sun, *ASP Conf. Ser.*, 223, 1057
- Schüssler, M. & Solanki, S. K. 1992, *A&A*, 264, L13
- Strassmeier, K. G. 2009, *A&A Rev.*, 17, 251